Depolarization Estimates from Linear H and V Measurements with Weather Radars Operating in Simultaneous Transmission–Simultaneous Receiving Mode

SERGEY Y. MATROSOV

Cooperative Institute for Research in the Environmental Sciences, University of Colorado, and NOAA/Environmental Technology Laboratory, Boulder, Colorado

(Manuscript received 13 June 2003, in final form 13 October 2003)

ABSTRACT

Circular depolarization ratio (CDR) is a polarimetric parameter, which, unlike linear depolarization ratio (LDR), does not exhibit significant dependence on hydrometeor orientation and can be used for particle type identification and shape estimation if propagation effects are small. The measurement scheme with simultaneous transmission and simultaneous reception (STSR) of horizontally and vertically polarized signals is widely used with research and operational radars. The STSR scheme does not provide direct measurements of depolarization. This study presents an estimator to obtain depolarization ratios from STSR complex voltages in radar receivers. This estimator provides true CDR if the phase shift on transmission, β, is equal to $\pm 90^\circ$ and the phase shift on reception, γ, equals $-\beta$. Even if these conditions are not satisfied, depolarization estimates are still possible if $\beta + \gamma = 0^\circ$ (though such estimates deviate slightly from true CDR varying between CDR and slant-45°LDR). The sum $\beta + \gamma$ represents the initial differential phase shift offset and can be accounted for. The use of this depolarization estimator is illustrated with the data from the NOAA X-band radar. The measurements in ice clouds demonstrate the utility of near-CDR estimates to identify dendritic crystals and their gradual aggregation within the cloud. Illustrations are also given for near-CDR estimates in rain. An important advantage of depolarization estimates in the STSR mode is that these estimates are obtained from two ''strong'' channel returns. This greatly relaxes the radar sensitivity requirements compared to radar systems that utilize direct depolarization measurements as the power ratio of radar echoes measured in ''strong'' and ''weak'' receiving channels that represent two orthogonal polarizations.

1. Introduction

Polarimetric radars are a power tool for quantitative studies of properties of atmospheric hydrometeors (Doviak and Zrnic 1993; English et al. 1991; Bringi and Chandrasekar 2001). The majority of meteorological polarimetric radars employ the linear polarization basis defined by the horizontal (h) and the vertical (v) polarizations. Although some earlier (e.g., McCormick and Hendry 1975) and more recent (e.g., Krehbiel et al. 1996) studies of precipitation used radars operating in the circular polarization basis, this basis, defined by the left-hand circular (LHC) and right-hand circular (RHC) polarizations, has not become predominant in meteorological radars, in part because of a rather strong dependence of orthogonal radar echoes on propagation effects in rain.

Corresponding author address: Dr. Sergey Y. Matrosov, R/E/ET7, 325 Broadway, Boulder, CO 80305.
E-mail: Sergey.Matrosov@noaa.gov

However, in situations when propagation effects are small, polarimetric parameters in the circular basis contain valuable information on hydrometeor types and shapes. It has been shown (e.g., Matrosov 1991; Matrosov et al. 2001) that circular depolarization ratio (CDR) measurements can successfully be used to distinguish between layers of planar-type and columnar-type hydrometeors in winter clouds and to estimate their effective shape as characterized by the aspect ratio. Though a number of methods for identifying different species of hydrometeors in precipitating systems (i.e., rain of different intensity, hail, snow, cloud ice, etc.) use only linear polarimetric parameters, including the linear depolarization ratio (LDR; e.g., Vivekanandan et al. 1999; Zrnic and Ryzhkov 1999), circular-polarization-based approaches have an advantage because CDR provides information on particle shape and shows only a very modest dependence on particle orientation, while LDR depends very strongly on hydrometer orientation. Unraveling ef-

© 2004 American Meteorological Society

fects of shape and orientation in LDR is not straightforward. Furthermore, the depolarization is stronger in the circular basis than in traditional linear h–v basis (Matrosov 1991; Torlashi and Holt 1998). The National Oceanic and Atmospheric Administration (NOAA)/Environmental Technology Laboratory (ETL) studies of winter clouds using a Ka-band radar operating in the circular and closely related to the circular polarization bases (Matrosov et al. 1996, 2001; Reinking et al. 2002) lead to the concept of the Ground-Based Remote Icing Detection System (GRIDS) for identifying supercooled large liquid water drops in nonprecipitating or weakly precipitating winter clouds based on CDR measurements (Reinking et al. 2001). The GRIDS radar needs to be very sensitive and provide measurements over a very large dynamic range because ''weak'' polarization channel echoes in the case of near-spherical scatterers such as water drops are typically about 30 dB lower than echoes in the ''strong'' polarization channel.

The linear polarization basis, however, still remains the basis of choice for most research polarimetric radars that are used for precipitation studies. In the traditional measurements scheme, horizontally (h) and vertically (v) polarized radar signals are alternately transmitted using the fast polarization switch with one (Zrnic 1991) or two receivers. Either only copolar or both copolar and cross-polar echoes are received. In the latter case, the LDR measurements are available. Potentially, CDR estimates can be obtained from the polarimetric parameters in the linear basis under certain assumptions (Jameson 1987); however, it requires very accurate measurements of these parameters over a large dynamic range, and the resulting estimates could have high uncertainties due to the measurement noise. A version of the h–v polarization basis is a slant linear basis when the polarization plane of the transmitted radar signals is tilted by 45° relative to the horizontal (e.g., Chandrasekar et al. 1994; Chandra et al. 1995; Matrosov et al. 2001). If both 45° slant and −45° slant polarization components are received, the corresponding echo power measurements result in slant-45° LDR (SLDR). It can be shown that for noncanted scatterers CDR and SLDR are essentially identical. CDR is higher than SLDR if hydrometeors are canted. A number of ETL's Ka-band studies of winter clouds were conducted using SLDR (Reinking et al. 2002).

In recent years, another polarimetric measurement scheme has become increasingly popular. Under this scheme, the horizontally and vertically polarized radar signals are transmitted simultaneously and the return echoes on both polarizations are then simultaneously measured by two receivers (Holt et al. 1999; Doviak et al 2000, Torlashi and Gingras 2000; Scott et al. 2001). One receiver can also be used for a switched reception in the simultaneous transmission–alternate reception (STAR) mode. The simultaneous transmission and simultaneous receiving (STSR) measurement scheme offers a number of advantages compared to the traditional fast-switching scheme. These advantages are discussed in detail by Doviak et al. (2000). The STSR scheme was tested with the New Mexico Institute of Mining and Technology X-band radar (Scott et al. 2001) and the Colorado State University–University of Chicago–Illinois State Water Survey (CSU–CHILL) S-band radar. This scheme, sometimes referred to as a measurement scheme in a ''hybrid'' polarization basis (Bringi and Chandrasekar 2001), is chosen for the polarimetric upgrade of the Weather Surveillance Radar-1988 Doppler (WSR-88D) Next-Generation Weather Radar (NEXRAD) network (Doviak et al. 2000). The STSR scheme was also implemented with the NOAA/ETL X-band precipitation radar in 2000 (Martner et al. 2001). In projects prior to 2000, this radar was used in the fast-switch h–v mode with simultaneous receiving copolar and cross-polar echoes (Matrosov et al. 1999).

One important disadvantage of the STSR scheme is that it does not offer a direct measurement of depolarization, though depolarization estimates can still be obtained from the data (Holt et al. 1999). In this study, an estimator to derive for CDR and closely related depolarization ratios (e.g., SLDR) directly from measured complex voltages in the STSR scheme is discussed, and illustrations are given for depolarization estimates in ice clouds and rain obtained from measurements taken with the NOAA X-band radar.

2. Radar measurables

In the linear h–v basis, the components of the electric vector $[E_h, E_v]$ of transmitted radar signals exiting the antenna relate to components of radar echoes at the antenna terminals $[E_{ht}, E_{vt}]$ by means of the transformation amplitude matrix, which is represented by the scattering matrix bracketed by the two propagation matrices (Doviak et al. 2000):

$$\begin{vmatrix} E_{ht} \\ E_{vt} \end{vmatrix} = \begin{vmatrix} T_h & 0 \\ 0 & T_v \end{vmatrix} \begin{vmatrix} S_{hh} & S_{hv} \\ S_{hv} & S_{vv} \end{vmatrix} \begin{vmatrix} T_h & 0 \\ 0 & T_v \end{vmatrix} \begin{vmatrix} E_h \\ E_v \end{vmatrix}, \quad (1)$$

where nondiagonal terms in the scattering matrix are equal to each other in the radar convention, and the propagation matrix diagonal elements are given by

$$T_h = (\Delta A_h)^{0.5} \exp(-j\Phi_{DP}/2), \quad (2a)$$

$$T_v = (\Delta A_v)^{0.5}. \quad (2b)$$

These propagation elements are expressed using one-way power attenuations (ΔA_h) and (ΔA_v) and the round trip phase difference Φ_{DP} between the horizontal and vertical echo components. The amplitude scattering matrix elements describe the transformation of the electrical vector on backscattering. In the STSR scheme, $|E_h| = |E_v|$. Using (1) and assuming that the phase difference between horizontally and vertically trans-

mitted components is β and the phase difference in the h and v receivers is γ, one can express the complex voltages measured on h and v polarizations ($V_h^{(s)}$ and $V_v^{(s)}$) that are proportional to the elements E_{ht} and E_{vt} in this scheme:

$$V_h^{(s)} = \{S_{hh}A_{hv}\exp[j(-\Phi_{DP} + \beta + \gamma)] + S_{hv}A_{hv}^{0.5}\exp[j(-\Phi_{DP}/2 + \gamma)]\}c, \quad (3a)$$

$$V_v^{(s)} = \{S_{hv}A_{hv}^{0.5}\exp[j(-\Phi_{DP}/2 + \beta)] + S_{vv}\}c, \quad (3b)$$

where c is a constant, the superscript (s) refers to the STSR measurement scheme, and

$$A_{hv} = \Delta A_h/\Delta A_v. \quad (4)$$

For the fast h–v transmission switch and two-receiver scheme, the corresponding complex voltages are

$$V_h = S_{hh}A_{hv}\exp[j(-\Phi_{DP} + \beta + \gamma)]c, \quad (5a)$$

$$V_v = S_{vv}c, \quad (5b)$$

$$V_{vh} = S_{hv}A_{hv}^{0.5}\exp[j(-\Phi_{DP}/2 + \beta]c, \quad (5c)$$

where V_{vh} is the complex voltage for the cross-polar component if the h polarization is transmitted (note that in the convention adopted here $S_{hv} = S_{vh}$). The radar measurables traditionally estimated in the fast-transmission-switch scheme are differential reflectivity Z_{DR}, correlation coefficient ρ_{hv}, the differential phase shift Φ_{DP}, and linear depolarization ratio in linear units L_{dr}:

$$Z_{DR} = \langle|V_h|^2\rangle/\langle|V_v|^2\rangle, \quad (6a)$$

$$\rho_{hv} = |\langle V_hV_v^*\rangle|/(\langle|V_h|^2\rangle^{0.5}\langle|V_v|^2\rangle^{0.5}), \quad (6b)$$

$$\Phi_{DP} = \arg(\langle V_hV_v^*\rangle), \quad (6c)$$

$$L_{dr} = \langle|V_{vh}|^2\rangle/\langle|V_h|^2\rangle, \quad (6d)$$

where the angular brackets mean averaging over the hydrometeor size distribution function and orientations, * is the complex conjugate sign, and $\mathrm{LDR} = 10\log_{10}(L_{dr})$. Note that, given (6d), LDR is LDR_h here as opposed to LDR_v. The estimate of ρ_{hv} in this scheme is not done at zero lag time, and some correlation model needs to be assumed in order to recalculate estimates from (6b) for ρ_{hv} at zero lag time [i.e., $\rho_{hv}(0)$].

In the STSR scheme, estimates of differential reflectivity, correlation coefficient (at zero lag time), and differential phase shift are calculated using the following estimators:

$$Z_{DR}^{(s)} = \langle|V_h^{(s)}|^2\rangle/\langle|V_v^{(s)}|^2\rangle, \quad (7a)$$

$$\rho_{hv}^{(s)}(0) = \frac{|\langle V_h^{(s)}V_v^{(s)*}\rangle|}{(\langle|V_h^{(s)}|^2\rangle^{0.5}\langle|V_v^{(s)}|^2\rangle^{0.5})}, \quad (7b)$$

$$\Phi_{DP}^{(s)} = \arg(\langle V_h^{(s)}V_v^{(s)*}\rangle). \quad (7c)$$

Note that estimates of primary polarimetric parameters [(6a)–(6c)] and [(7a)–(7c)] in the fast-switch scheme and in the STSR scheme are not identical. The corresponding differences are not expected to be substantial and they usually are ignored (Doviak et al. 2000). However, the fact that polarimetric parameters in different measurement schemes are not identical should be retained. It was shown (Humphries et al. 1991) that for canting angles not exceeding 2° differences between $Z_{DR}^{(s)}$ and Z_{DR} can be neglected; however, for canting angles of about 10° these differences can reach a few tenths of a decibel (Matrosov et al. 2002). Scott et al. (2001) also discussed differences between $\rho_{hv}^{(s)}$ and ρ_{hv}.

The STSR measurement scheme does not allow direct measurements of depolarization; however, the depolarization information is contained in the STSR polarimetric measurements. A simple estimator can be suggested for estimating depolarization from the measured complex voltages. It can be shown that the LHC and RHC radar echoes can be expressed in terms of the matrix elements (1) (Doviak et al. 2000)

$$\mathrm{RHC} \sim (S_{hh}T_h^2 + S_{vv}T_v^2) \quad \text{(LHC transmitted)}, \quad (8a)$$

$$\mathrm{LHC} \sim (S_{hh}T_h^2 + S_{vv}T_v^2) \quad \text{(RHC transmitted)}, \quad (8b)$$

$$\mathrm{LHC} \sim (S_{hh}T_h^2 - S_{vv}T_v^2 + 2jS_{hv}T_hT_v) \quad \text{(LHC transmitted)}, \quad (8c)$$

$$\mathrm{RHC} \sim (S_{hh}T_h^2 - S_{vv}T_v^2 - 2jS_{hv}T_hT_v) \quad \text{(RHC transmitted)}. \quad (8d)$$

Using (2a), (2b), and (4), CDR can be written as a ratio of (8c) and (8a) or (8d) and (8b):

$$C_{dr} = \frac{\langle|S_{hh}A_{hv}\exp(-j\Phi_{DP}) \pm 2jS_{hv}A_{hv}^{0.5}\exp(-j\Phi_{DP}/2) - S_{vv}|^2\rangle}{\langle|S_{hh}A_{hv}\exp(-j\Phi_{DP}) + S_{vv})|^2\rangle}, \quad (9)$$

$$\mathrm{CDR} = 10\log_{10}(C_{dr}). \quad (9a)$$

The following depolarization estimator in the STSR scheme can be used:

$$D_{dr}^{(s)} = \langle|V_h^{(s)} - V_v^{(s)}|^2\rangle/\langle|V_h^{(s)} + V_v^{(s)}|^2\rangle, \quad (10)$$

$$\mathrm{DR}^{(s)} = 10\log_{10}[D_{dr}^{(s)}]. \quad (10a)$$

Taking into account (3a) and (3b), (10) can be rewritten as

$$D_{\mathrm{dr}}^{(s)} = \frac{\langle |S_{hh}A_{hv}\exp[j(-\Phi_{DP}+\beta+\gamma)] + S_{hv}A_{hv}^{0.5}\exp[j(-\Phi_{DP}/2+\gamma)] - S_{hv}A_{hv}^{0.5}\exp[j(-\Phi_{DP}/2+\beta)] - S_{vv}|^2\rangle}{\langle |S_{hh}A_{hv}\exp[j(-\Phi_{DP}+\beta+\gamma)] + S_{hv}A_{hv}^{0.5}\exp[j(-\Phi_{DP}/2+\gamma)] + S_{hv}A_{hv}^{0.5}\exp[j(-\Phi_{DP}/2+\beta)] + S_{vv}|^2\rangle}. \quad (11)$$

If $\gamma = -\beta = \pm 90°$, (11) provides true CDR. Indeed, for $\gamma = -\beta = \pm 90°$, the circularly polarized signals are transmitted and, with one receiver having an additional 90° phase shift, RHC and LHC return echo components are measured. The nominators and denominators in (9) and (11) describe the ''weak'' and ''strong'' polarization returns (if $\Phi_{DP} < 90°$).

The sum $\gamma + \beta$ has a simple manifestation in polarimetric measurements of differential phase shift: it represents an initial phase (in other words, a phase offset) in measurements of Φ_{DP} as a function of range. If the initial backscatter shift can be neglected (e.g., at vertical viewing, small drops), this holds exactly when the estimator (6c) is used and approximately (unless the cross terms S_{hv} are zero, as in drizzle) when the estimator (7c) is used for phase estimates. This initial phase can be determined simply from measurements in rain. More statistical reliability can be achieved when pointing radar vertically, since in such geometry there is practically no differential phase shift accumulation along the radar beam. This phase sum can potentially be adjusted by tuning the receiver and/or transmitter hardware. It was established that the NOAA/ETL X-band radar, used in recent field projects, has $\gamma + \beta \approx 3°$–$4°$, although the individual values of γ and β were not exactly known. Once set, the phases γ and β can, most likely, be assumed constant. An indirect indication of this is the fact that the phase offset $\gamma + \beta$ in the NOAA/ETL X-band radar did not exhibit noticeable variability in the course of field measurements.

As soon as the sum $\gamma + \beta$ is sufficiently small or accounted for in data processing, the estimator [(10)–(11)] can be used for approximate depolarization measurements, even if the condition $\gamma = -\beta = \pm 90°$ does not hold true. The arguments in favor of this are similar to the ones given by Doviak et al. (2000), who pointed out that the differences in the STSR mode and the fast-switching mode estimates of differential reflectivity, copolar correlation coefficient, and differential phase shift can be neglected for the most practical cases. These arguments rely on the notion that the cross-polar terms containing S_{hv} are expected to be significantly smaller than copolar terms containing S_{hh} and S_{vv} for most atmospheric hydrometeors. Such arguments, however, could be less powerful for quasi-spherical particles since the difference between S_{hh} and S_{vv} [see the numerator in (11)] is small and the relative importance of the cross-polar terms is increasing. Given this, it is highly desirable for CDR estimates to have $\gamma \approx -\beta \approx \pm 90°$. If $\gamma \approx \beta \approx 0°$, (11) provides SLDR as defined by Chandrasekar et al. (1994). For values other than $\pm 90°$ or 0°, depolarization from (11) corresponds to some elliptical polarization providing ratios between CDR and SLDR. As shown by Matrosov et al. (2001), for hydrometeors that are aligned with their major dimensions, preferably in the horizontal plane, differences between CDR and SLDR (and elliptical depolarization ratios mentioned above) are expected to be small.

3. Examples of estimating depolarization in ice clouds

As mentioned before, CDR (and, very closely related to it, SLDR) is a useful polarimetric parameter for identifying hydrometeor types and estimating their shapes. Most single-shape ice hydrometeors (except quasi-spherical ones) tend to be preferably oriented with their major dimensions in the horizontal plane (e.g., Sassen 1980). It has been shown both theoretically and experimentally (e.g., Matrosov 1991; Matrosov et al. 2001) that planar-type ice crystals, such as dendrites, stellars, and different kinds of pristine plates, show a very distinct CDR pattern as a function of the radar elevation angle χ. CDR values from such crystals are the highest at small elevation angles. As χ increases, CDR monotonically decreases, reaching its minimum values when the radar beam is pointing vertically. The dynamic range of CDR variations as a function of the radar elevation angle depends on the hydrometeor mean aspect ratio and the degree of particle flutter around the horizontal orientation. CDR values, observed when χ is about 30°–40°, can be used for estimating the hydrometeor mean aspect ratio if an assumption about the bulk density is made (Matrosov et al. 2001).

The depolarization ratios of columnar-type crystals (e.g., columns, bullets, needles) exhibit almost no change (in SLDR) or a slight increase (in CDR) when χ increases. As in the case of planar crystals, mean-aspect-ratio estimates can be made based on depolarization measurements. Measurements made with the NOAA Ka-band radar (Reinking et al. 2002) also showed that lightly aggregated ice hydrometeors still retain depolarization patterns that are characteristic of pristine planar or columnar-type crystals, though these patterns are not very profound. Depolarization of heavily aggregated ice hydrometeors and highly irregular particles is characterized by very low values that exhibit no or very little variability with χ. Matrosov et al. (2001) and Reinking et al. (2002) show many examples of SLDR measurements in winter clouds that support the

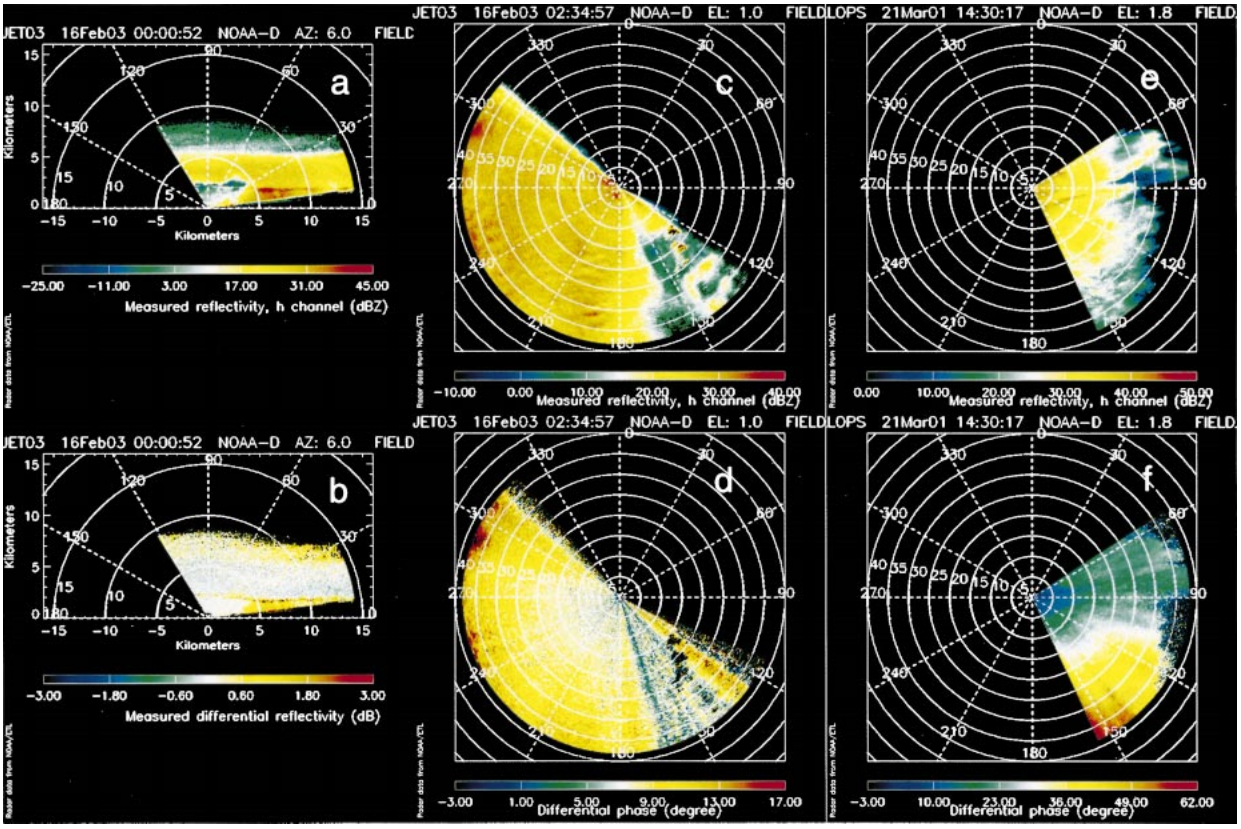

FIG. 1. RHI scans (azimuth angle 6°) of (a) horizontal polarization reflectivity and (b) differential reflectivity at 0001 UTC 16 Feb 2003. Azimuthal scans (elevation angle 1°) of (c) horizontal polarization reflectivity and (d) differential phase shift in light rain at 0235 UTC 16 Feb 2003. Azimuthal scans (elevation angle 1°) of (e) horizontal polarization reflectivity and (f) differential phase shift in moderate-to-heavy rain at 0235 UTC 21 Mar 2001. All measurements are from the NOAA/ETL X-band radar (STSR mode).

information stated above. The polarization used in those measurements was very close to the 45°-slant linear, and two receivers were used for simultaneous recording of the copolar and cross-polar returns.

Depolarization measurements in nonprecipitating and weakly precipitating winter clouds require very sensitive radars, such as the NOAA/ETL Ka-band radar (Martner et al. 2002), since the radar returns in the ''weak'' channel are usually two to three orders of magnitude below the ''strong'' channel returns. The approach suggested above to estimate depolarization that is close to CDR (or SLDR, depending on the hardware phases β and γ) using the STSR measurement scheme that utilizes two ''strong'' copolar returns significantly eases radar sensitivity requirements and allows the use of longer wavelength radars, which also alleviates the propagation effects.

Figures 1a and 1b show a range–height indicator (RHI) scan of a cloud observed by the NOAA/ETL X-band radar, which is about three orders of magnitude less sensitive than the NOAA/ETL Ka-band radar. The observation was made during the Pacific Jets Experiment in January–February 2003 (PACJET-03). The radar was located at the coast near Fort Ross, California. There is very little or no rain-present below the cloud for $30° < \chi < 120°$. However, rain is present north of the radar at $\chi \lesssim 30°$, as can be seen from the 6° azimuth RHI in Fig. 1a, and the melting-layer bright band near 2-km height indicates the presence of ice in the cloud above that altitude.

Figure 2 shows the elevation-angle dependencies of $Z_{\mathrm{DR}}^{(s)}$ and $\mathrm{DR}^{(s)}$ obtained using estimators (7a) and (10) for a constant height of 5.5 km from the RHI scan of Fig. 1. This height corresponds to a transition zone between low-reflectivity and high-reflectivity echoes inside the cloud. Radar echoes above 5.5 km are too close to the radar noise floor for reliable estimates of $\mathrm{DR}^{(s)}$. As was mentioned before, the estimated value for $\gamma + \beta$ was about 3°–4°. To correct for this offset, the complex voltage terms $V_h^{(s)}$ (3a) were multiplied by a factor $\exp(-j3.5°\pi/180°)$. No information on individual values of γ and β was available, and no attempt was made to one individual values of these angles. As discussed above, however, estimates of $\mathrm{DR}^{(s)}$ are expected to correspond to CDR or SLDR or somewhere in between these two ratios, depending on individual values of γ and β. Such uncertainty in depolarization basis can probably be tolerated since, as mentioned above, the

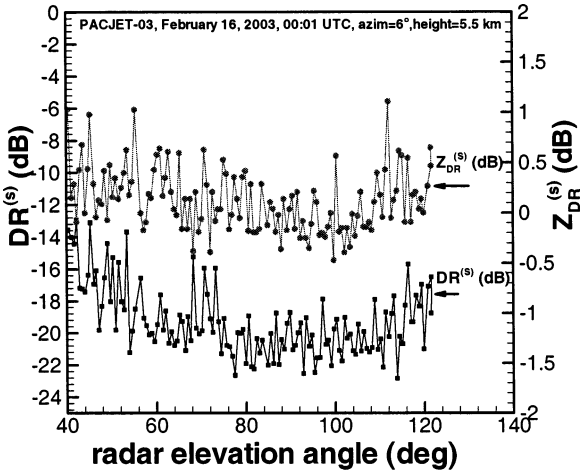

FIG. 2. Elevation-angle dependencies of $DR^{(s)}$ and $Z_{DR}^{(s)}$ in the ice cloud shown in Figs. 1a and 1b. Estimates correspond to a constant height of 5.5 km.

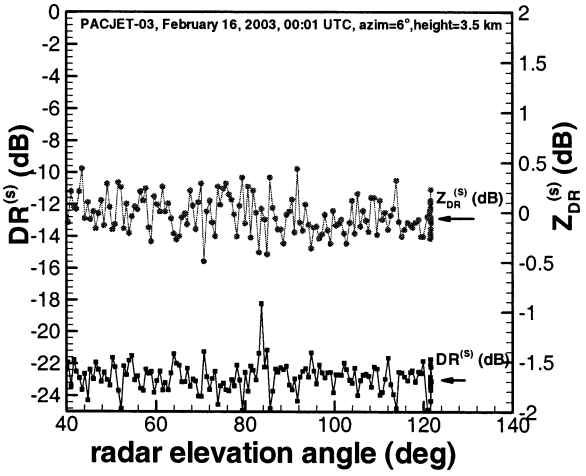

FIG. 3. Elevation-angle dependencies of $DR^{(s)}$ and $Z_{DR}^{(s)}$ in the ice cloud shown in Figs. 1a and 1b. Estimates correspond to a constant height of 3.5 km.

corresponding differences are expected to be small. No significant accumulation of the differential phase shift $\Phi_{DP}^{(s)}$ along the radar beams in the RHI scan in Fig. 2 was observed for $30° < \chi < 120°$ (not shown), so the propagation effects were neglected for this case.

It can be seen in Fig. 2 that $DR^{(s)}$ as a function of χ exhibits a typical pattern for CDR and SLDR that is characteristic of planar crystals. The decreasing trend of depolarization between $\chi = 40°$ and $\chi = 90°$ is about 4–5 dB, which is indicative of rimed dendrites (Fig. 5 in Matrosov et al. 2001) or lightly aggregated dendrites (Fig. 11 in Reinking et al. 2002). Though much less profound than that for $DR^{(s)}$, $Z_{DR}^{(s)}$ as a function of χ shows a somewhat similar trend. The corresponding variability in $Z_{DR}^{(s)}$ is only a few tenths of a decibel. Although differential reflectivity and circular depolarization ratio are not completely independent parameters, CDR as mentioned above does not depend on particle orientation in the polarization plane, whereas differential reflectivity does. It should be mentioned also that, unlike for depolarization measurements, analyzing the $Z_{DR}^{(s)}$ elevation-angle trend does not allow discrimination between planar and columnar crystals (Matrosov et al. 2001). The statistical variability of $DR^{(s)}$ estimates shown here (around 1 dB) is similar to that observed with direct depolarization measurements using the NOAA/ETL Ka-band radar.

Figure 3 shows the $DR^{(s)}$ and $Z_{DR}^{(s)}$ as functions of χ for a constant cloud height of 3.5 km, which corresponds to the area of high reflectivity. It can be seen that both $DR^{(s)}$ and $Z_{DR}^{(s)}$ do not exhibit any obvious elevation-angle trend, and $Z_{DR}^{(s)}$ is close to zero. This, most likely, corresponds to highly aggregated irregular ice hydrometeors. It can be suggested that dendrites gradually become more aggregated as they fall from higher to lower altitudes within the cloud. The bulk density of highly aggregated particles is relatively low, so they do not exhibit noticeable polarimeric signatures.

The $DR^{(s)}$ level of around -23 dB is several decibels higher than the level of about -27 to -28 dB seen for such scatterers with the NOAA/ETL Ka-band radar (Matrosov et al. 2001; Reinking et al. 2002). One possible explanation for this difference for low $DR^{(s)}$ values can be a rather mediocre polarization isolation of the X-band radar antenna, which was not designed specifically for polarimetric measurements. However, fine-tuning radar hardware parameters, including hardware phases β and γ to optimize polarimetric performance, will require substantial efforts in the future but is not crucial to the arguments presented here.

Another important advantage of depolarization estimates in the STSR scheme, aside from the ability of getting depolarization estimates in the strong receiving channel measurement mode, is the possibility of assessing the propagation effects. In a single-depolarization measurement mode employed by the NOAA/ETL Ka-band radar and the future GRIDS radar (i.e., transmitting single polarization and receiving co- and cross-polarized echos), there is no simple way of estimating these effects, although one can assume that for some clouds observed at Ka-band, these effects can be substantial. The STSR mode offers a way of doing so because it provides a differential phase shift measurement that is related to the magnitude of propagation effects.

To illustrate this point, Fig. 4 shows model calculations of CDR (in the Rayleigh regime) for the dendritic crystals viewed at $\chi = 40°$ (i.e., the angle suggested for the GRIDS radar). Absorption in a pure ice phase can be neglected; hence, the propagation effects are solely due to the phase rotation. The phase rotation causes CDR to increase with Φ_{DP}. Also shown in this figure is the difference:

$$\Delta C_{\mathrm{dr}}(\Phi_{DP}) = C_{\mathrm{dr}}(\Phi_{DP}) - C_{\mathrm{dr}}(\Phi_{DP} = 0). \quad (12)$$

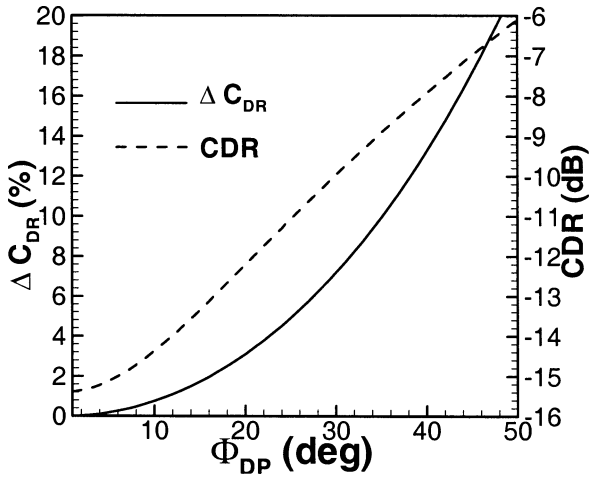

FIG. 4. Model calculations of CDR and ΔC_{DR} as functions of the differential phase shift for the model of single pristine dendrites oriented in the horizontal plane and viewed at 40° elevation angle.

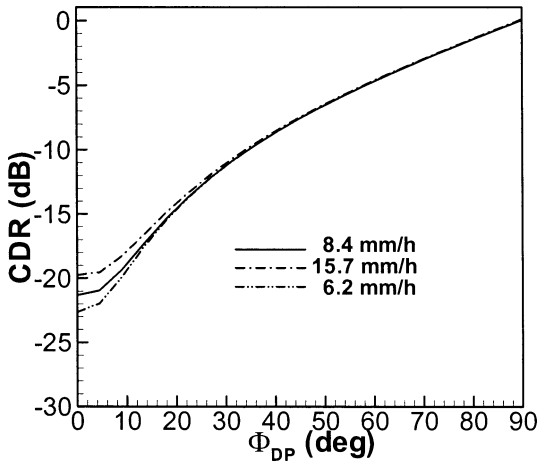

FIG. 5. Model calculations of CDR as a function of the differential phase shift in rain for three different experimental drop size distributions.

It can be seen that for some practical cases, the propagation effects can be neglected if $\Phi_{DP} < 10°$, but they need to be accounted for at higher differential phase shift values. The development of the procedure to comprehensively correct for the propagation effects is beyond the scope of current research.

4. Examples of estimating depolarization in rain

Circular polarization radar measurements have not been used extensively for rain studies mainly because of the significant dependence of reflectivities and hence CDR on propagation effects (Doviak et al. 2000). Compared to rain radars operating at S and C bands, these effects are even more profoundly manifested at shorter radar wavelengths, such as those at X band. In spite of these limiting issues, testing the suggested $DR^{(s)}$ estimator in rain is instructive since the results can be compared to the theoretical expectations, thus confirming the robustness of this estimator. The NOAA/ETL X-band radar collected a significant amount of rain data in the STSR measurement scheme that can be used for this purpose. Note also that X-band frequencies have been shown to be quite valuable in the rainfall parameter retrieval using measurements of differential phase shift. These measurements offer a robust way of accounting for the effects of partial attenuation in the linear polarization basis reflectivities (Matrosov et al. 1999, 2002).

Figure 5 shows model calculations of CDR measurements in rain as a function of differential phase shift Φ_{DP}. Three different experimental drop size distributions (DSDs) collected during the PACJET-03 project with a Joss–Waldfogel raindrop disdrometer were used for this illustration. It was assumed that the rain microphysical properties were the same along the propagation path and in the radar resolution volume. The presented data demonstrate the significance of propagation effects on CDR in rain. The calculations were performed with accounting for both differential phase shift on propagation and differential attenuation between h and v components using the T-matrix approach (Barber and Yeh 1975). The equilibrium drop shape model and the drop temperature of 10°C were assumed. For a given drop shape model, the effects of differential phase shift and differential attenuation are directly related, so CDR dependence on propagation effects can be given as a function of Φ_{DP}.

As Φ_{DP} increases (Fig. 5) the return echo power gradually shifts from the cross-polar circular polarization component (in the ''strong'' channel) to the copolar component (in the ''weak'' channel), and CDR increases. At $\Phi_{DP} \approx 90°$, both components are of equal strength. For $\Phi_{DP} > 90°$ (but $\Phi_{DP} < 270°$) the meanings of the ''strong'' and ''weak'' channels become reversed. At $\Phi_{DP} = 180°$ in uniform rain, the measured CDR is the negative of true CDR. The differences in CDR in rain are important at small values of Φ_{DP}, where propagation effects are not yet strong. In this case, CDR values are directly related to the drop shapes since these depolarization ratios (unlike LDR and, to the lesser extent, Z_{DR}) are invariant to the drop orientation in the polarization plane. The separation between backscattering and propagation effects affecting CDR was discussed by Torlashi and Holt (1993). Unraveling these effects becomes progressively more difficult as the accumulated differential phase shift increases.

Figure 6 shows estimates of $\Phi_{DP}^{(s)}$ and $DR^{(s)}$ as functions of range in a light stratiform rain with intensity of about 2–3 mm h^{-1}. The radar beam for which data are shown corresponds to the azimuth 270° in the azimuthal scan presented in Figs. 1c and 1d. The data were collected during the PACJET-03 field tests about 1.5 h after the RHI scans discussed in section 3. It can be seen that a differential phase offset (i.e., the sum $\beta + \gamma$) is about 3°–4°, as mentioned above. The thick solid

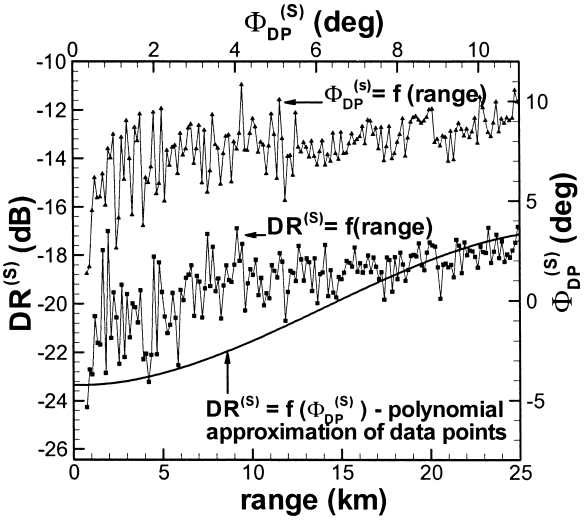

FIG. 6. Estimates of $DR^{(s)}$ and $\Phi_{DP}^{(s)}$ in a light rain as functions of range. The data correspond to the 270° azimuthal angle in Figs. 1c and 1d. The approximation $DR^{(s)} = f(\Phi_{DP}^{(s)})$ (solid line) should be read relative to the upper x axis.

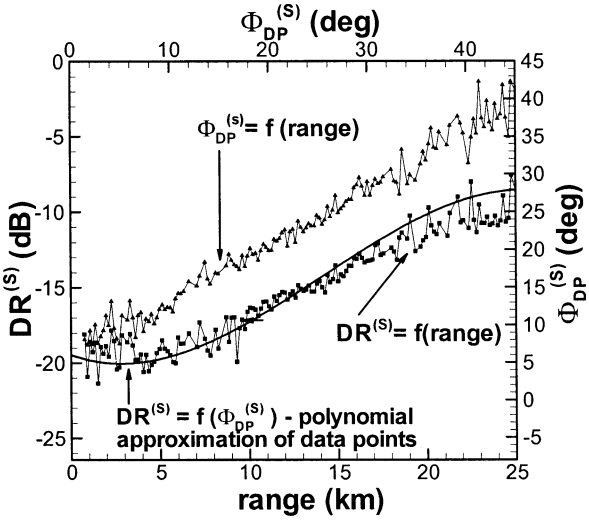

FIG. 7. Estimates of $DR^{(s)}$ and $\Phi_{DP}^{(s)}$ in a moderate-to-heavy rain as functions of range. The data correspond to the 134° azimuthal angle in Figs. 1e and 1f. The approximation $DR^{(s)} = f(\Phi_{DP}^{(s)})$ (solid line) should be read relative to the upper x axis.

line in Fig. 6 shows estimates of $DR^{(s)}$ as a function of $\Phi_{DP}^{(s)}$ estimates (plotted as the upper x axis). Since both $DR^{(s)}$ and $\Phi_{DP}^{(s)}$ are noisy, this correspondence is approximated by a polynomial curve. The polynomial approximation $DR^{(s)} = f(\Phi_{DP}^{(s)})$does not necessarily follow the $DR^{(s)} = f(range)$ data points since $\Phi_{DP}^{(s)}$ as a function of range is not generally linear. The main purpose of showing $DR^{(s)} = f(\Phi_{DP}^{(s)})$data approximation is to compare it with the theoretical curves in Fig. 5. As one can see, the $DR^{(s)}$ increase as a function of differential phase shift is in general agreement with the theoretical predictions for CDR presented in Fig. 5. Although, as mentioned above, there is an uncertainty about the polarization basis of $DR^{(s)}$ estimates (since individual values of the hardware phases γ and β were not known), these depolarization estimates in rain are expected to be close to CDR because canting of rain drops is generally small, which results in cross-polar terms S_{hv} being very small, and CDR and SLDR being close.

An example of $DR^{(s)}$ estimates from (10) for a moderate/heavy rain is shown in Fig. 7. Since only relatively light rains were observed during PACJET-03, data from an earlier field project conducted at Wallops Island, Virginia, in the spring of 2001 (Matrosov et al. 2001) are used here for the illustration. The radar hardware was the same as in PACJET-03. It was established that during the Wallops experiment, the differential phase offset (i.e., $\beta + \gamma$) was also about 3°–4°, as in the PACJET-03 dataset, so the same procedure [i.e., the multiplication of the complex voltage term $V_h^{(s)}$ (3a) by a factor $\exp(-j3.5°\pi/180°)$], was used to obtain estimates of $DR^{(s)}$.

The radar beam data shown in Fig. 7 correspond to the 135° azimuth in the sector scan shown in Figs. 1e and 1f. An average rainfall rate along the beam was about 20–25 mm h^{-1}. Radar signals at X-band frequencies are noticeably attenuated in rain of such intensity, as is evident from Fig. 1e, where measured (i.e., not corrected for attenuation) reflectivities on horizontal polarization are shown. A differential phase shift increase of about 40° over the 25-km range is observed. As shown in Fig. 5, such a phase shift corresponds to CDR values of about −9 to −10 dB, which generally agrees with the $DR^{(s)}$ estimates shown in Fig. 7. For this example, $DR^{(s)} = f(\Phi_{DP})$ and $DR^{(s)} = f$(range) are similar because Φ_{DP} as a function of range tends to be rather linear.

Figure 8 shows an example of $DR^{(s)}$ estimates in a

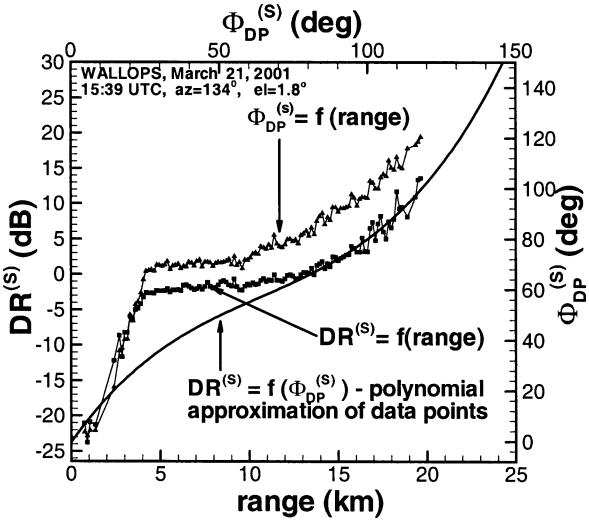

FIG. 8. Estimates of $DR^{(s)}$ and $\Phi_{DP}^{(s)}$ in a very heavy rain as functions of range. The approximation $DR^{(s)} = f(\Phi_{DP}^{(s)})$(solid line) should be read relative to the upper x axis.

very heavy rain. The radar signals penetrate a cell (from 1 km to about 4 km) of rain with an intensity of about 100 mm h^{-1}. Such intensity was indicated by at a Joss–Waldvogel disdrometer and a high-resolution (0.01 in.) tipping-bucket-type rain gauge that was recording tips every 8–9 s. Both the disdrometer and the gauge were deployed at 3.4 km from the radar along the 134° azimuth for which the data in Fig. 8 are shown. The differential phase shift accumulated in this cell is about 60°, which corresponds to the specific differential phase shift K_{DP} of about 15° km^{-1}. This cell of the very heavy rain is followed by a very light rain (from about 4 km to about 10 km) with a flat interval of $\Phi_{DP}^{(s)}$ and $DR^{(s)}$. The rain picks up again after a range of 10 km, and the radar signals are completely attenuated out beyond about 20 km when $\Phi_{DP}^{(s)}$ is reaching 120°. The NOAA/ETL X-band radar was not operating in its most sensitive mode during this field experiment.

As seen from Fig. 8, $DR^{(s)}$ estimates, as expected (see Fig. 5), are about 0 dB when $\Phi_{DP}^{(s)} \approx 90°$, signifying the equality of power received on two orthogonal components of the circular polarization. A ''switch'' between the ''strong'' and ''weak'' channels occurs at this point. One remarkable fact of differential phase shift measurements shown in Figs. 6–8 is that there are no obvious manifestations of the backscatter phase shift. Some possible explanations for this fact are discussed by Matrosov et al. (2002). Overall, the estimates of $DR^{(s)}$ in rain indicate a general robustness of the estimator (10), and they are in qualitative and, to a certain extent, quantitative agreement with the theoretical expectations for CDR.

5. Conclusions

The simultaneous transmission–simultaneous receiving (STSR) measurement scheme in the linear h–v basis is becoming increasingly popular with weather research polarimetric radars and is being considered for the polarimetric upgrade of the U.S. operational network of WSR-88D (NEXRAD) radars. Though this scheme offers a number of important advantages and a relative simplicity in hardware compared to the traditional fast-switching h–v mode, it does not provide a means for obtaining linear depolarization ratio (LDR), which is often measured by research polarimetric radars employing the fast-switching measurement scheme. The STSR scheme, however, does offer a relatively straightforward way for estimating circular depolarization ratio (CDR) and closely related depolarization ratios such as SLDR. For limited propagation effects (e.g., in nonprecipitating and weakly precipitating winter clouds) CDR is superior to LDR because it depends only weakly on hydrometeor orientation, whereas LDR shows a strong dependence on orientation; hence, CDR is more indicative of particle shape than LDR. Further more, CDR is greater than LDR in absolute terms. Thus a technique that allows CDR to be estimated in the STSR radar configuration adds a benefit of improved particle classifications.

A simple estimator that uses measurements of complex voltages V_h and V_v in h and v receiver channels in the STSR scheme directly provides depolarization values. The estimates depend on two differential phases of radar hardware: the differential phase between h and v components on transmission (β) and that on receiving (γ). When $\gamma = -\beta = \pm 90°$, these estimates represent true CDR and are subject to weather influences only. They are affected by propagation effects in the hydrometeor medium. Since γ and β individually contaminate the smaller cross-polar contributions to larger copolar echoes in the estimator, acceptable estimates of CDR are possible to obtain even if individual values of hardware phases are not exactly known, as long as the condition $\gamma + \beta = 0°$ is satisfied. For conditions other than $\gamma = -\beta = \pm 90°$, depolarization ratios, strictly speaking, correspond to other depolarization ratios (including SLDR for $\gamma = \beta = 0°$). The differences between CDR and these depolarization ratios, however, are small under the condition that cross-polar terms in the linear scattering matrix are small compared to copolar terms. This condition is often satisfied for planar and elongated ice crystals and rain drops that exhibit small canting. Though there is a potential for estimating CDR from measurements of other polarimetric parameters, the estimates directly from measured complex voltages are considered more robust.

An important advantage of such estimates is that the voltages from two linear copolar returns are used without a need for measuring ''weak''-channel polarization echoes. This significantly eases the sensitivity requirements for radars such as GRIDS that rely on CDR measurements. Thus, weaker transmitters, smaller antennas, or longer wavelengths could be used for such radars. Another important advantage of estimating CDR in the STSR measurement scheme is that the independent estimates of the meteorological differential phase shift ($\Phi_{DP}^{(s)}$) in this scheme can be used for assessing (and prospectively removing) the propagation effects from CDR estimates.

The $DR^{(s)}$ estimator providing near-CDR estimates in the STSR linear basis measurement scheme was initially tested using measurements of NOAA/ETL X-band radar in ice clouds and in rainfall of different intensities. The estimated value of the sum $\gamma + \beta$ for this radar was about 3°–4°, and a corresponding correction was introduced. No independent estimates of individual values for γ and β were available. The $DR^{(s)}$ data decreasing with an increase in the radar elevation angle χ were obtained for upper parts of ice clouds. These depolarization patterns are typical for CDR and SLDR of dendritic ice crystals, and they had been earlier observed with much more sensitive radars (e.g., the NOAA/ETL Ka-band radar) that were transmitting a single polarization and receiving the copolar and cross-polar components of return echoes. The $DR^{(s)}$ elevation angle pat-

terns are much more pronounced than those from differential reflectivity, and, unlike $Z_{DR}^{(s)}$, $DR^{(s)}$ can be used to differentiate between planar- and columnar-type ice crystals.

The $DR^{(s)}$ estimates in rain were in general qualitative and quantitative agreement with modeling. For small values of $\Phi_{DP}^{(s)}$, circular depolarization ratios are directly related to drop shapes. With increasing differential phase shift, $DR^{(s)}$ increases, reaching zero at $\Phi_{DP}^{(s)} \approx 90°$. Although initial tests indicated robustness of the $DR^{(s)}$ estimator, more data, obtained with different radars operating in the STSR mode in wider meteorological conditions, are needed to further verify this approach and explore its strengths and limitations. It is intended also to set $\gamma = -\beta = 90°$ (or $-90°$) with the NOAA/ETL X-band radar, so $DR^{(s)}$ will more closely correspond to CDR.

Acknowledgments. The author acknowledges useful discussions with S. Sekelsky, V. Melnikov, A. Ryzhkov, C. Campbell, B. Martner, and K. Clark. C. Campbell and I. Djalalova helped with the time series processing of the radar data from the NOAA/ETL X-band radar. Comments from two anonymous reviewers helped to improve manuscript. The X-band radar operations were funded by NOAA/ETL for PACJET-03 and by NASA's AMSR program for the Wallops Island experiment. Parts of this study were funded by the Federal Aviation Administration (FAA) through the GRIDS project.

REFERENCES

Barber, P., and C. Yeh, 1975: Scattering of electromagnetic waves by arbitrarily shaped dielectric bodies. *Appl. Opt.,* **14,** 2864–2872.

Bringi, V. N., and V. Chandrasekar, 2001: *Polarimetric Doppler Weather Radar*. Cambridge University Press, 636 pp.

Chandra, M., S. J. Wood, S. Lux, A. R. Holt, and A. Schroth, 1995: The PADRE Project. *COST 75 Weather Radar Systems,* C. G. Collier, Ed., European Commission, Rep. EUR 16013 EN, 507–518.

Chandrasekar, V., J. Hubbert, V. N. Bringi, and P. Meishner, 1994: Analysis and interpretation of dual-polarized radar measurements at +45° and −45° linear polarization basis. *J. Atmos. Oceanic Technol.,* **11,** 323–336.

Doviak, R. J., and D. S. Zrnić, 1993: *Doppler Radar and Weather Observations.* Academic Press, 562 pp.

——, V. Bringi, A. Ryzhkov, A. Zahrai, and D. Zrnic, 2000: Considerations for polarimetric upgrades to operational WSR-88D radars. *J. Atmos. Oceanic Technol.,* **17,** 257–278.

English, M., B. Kochtubajda, F. D. Barlow, A. R. Holt, and R. McGuinnes, 1991: Radar measurements of rainfall by differential propagation phase: A pilot experiment. *Atmos.–Ocean,* **29,** 357–380.

Holt, A. R., V. N. Bringi, and D. Brunkow, 1999: A comparison between parameters obtained with the CSU–CHILL radar from simultaneous and switched transmission of vertical and horizontal polarization. Preprints, *29th Conf. on Radar Meteorology,* Montreal, QC, Canada, Amer. Meteor. Soc., 214–217.

Humphries, R. G., A. R. Holt, and P. L. Smith, 1991: A radar configuration for monopulse differential reflectivity measurements. Preprints, *25th Conf. on Radar Meteorology,* Paris, France, Amer. Meteor. Soc., 622–625.

Jameson, A. R., 1987: Relations among linear and circular polarization parameters measured in canted hydrometeors. *J. Atmos. Oceanic Technol.,* **4,** 634–645.

Krehbiel, P., T. Chen, S. McCrary, W. Rison, G. Gray, and M. Brook, 1996: The use of dual channel circular polarization radar observations for remotely sensing storm electrification. *Meteor. Atmos. Phys.,* **59,** 65–82.

Martner, B. E., K. A. Clark, S. Y. Matrosov, W. C. Campbell, and J. S. Gibson, 2001: NOAA/ETL's polarization-upgraded X-band ''HYDRO'' radar. Preprints, *30th Int. Conf. on Radar Meteorology,* Munich, Germany, Amer. Meteor. Soc., 102–103.

——, B. W. Bartram, J. S. Gibson, W. C. Campbell, R. F. Reinking, and S. Y. Matrosov, 2002: An overview of NOAA/ETL's scanning Ka-band cloud radar. Preprints, *16th Conf. on Hydrology,* Orlando, FL, Amer. Meteor. Soc., 21–23.

Matrosov, S. Y., 1991: Theoretical study of radar polarization parameters obtained from cirrus clouds. *J. Atmos. Sci.,* **48,** 1062–1070.

——, R. F. Reinking, R. A. Kropfli, and B. W. Bartram, 1996: Estimation of ice hydrometeor types and shapes from radar polarization measurements. *J. Atmos. Oceanic Technol.,* **13,** 85–96.

——, R. A. Kropfli, R. F. Reinking, and B. E. Martner, 1999: Prospects for measuring rainfall using propagation differential phase in X- and Ka-radar bands. *J. Appl. Meteor.,* **38,** 766–776.

——, R. F. Reinking, R. A. Kropfli, B. E. Martner, and B. W. Bartram, 2001: On the use of radar depolarization ratios for estimating shapes of ice hydrometeors in winter clouds. *J. Appl. Meteor.,* **40,** 479–490.

——, K. A. Clark, B. E. Martner, and A. Tokay, 2002: X-band polarimetric radar measurements of rainfall. *J. Appl. Meteor.,* **41,** 941–952.

McCormick, G. C., and A. Hendry, 1975: Principles for the radar determination of the polarization properties for precipitation. *Radio Sci.,* **10,** 421–434.

Reinking, R. F., and Coauthors, 2001: Concept and design for a pilot demonstration Ground-based Remote Icing Detection System. Preprints, *30th Conf. on Radar Meteorology,* Munich, Germany, Amer. Meteor. Soc., 214–217.

——, S. Y. Matrosov, R. A. Kropfli, and B. W. Bartram, 2002: Evaluation of a 45° slant quasi-linear radar polarization state for distinguishing drizzle droplets, pristine ice crystals, and less regular ice particles. *J. Atmos. Oceanic Technol.,* **19,** 296–321.

Sassen, K., 1980: Remote sensing of planar ice crystal fall attitudes. *J. Meteor. Soc. Japan,* **58,** 422–429.

Scott, R. D., P. R. Krehbel, and W. Rison, 2001: The use of simultaneous horizontal and vertical transmissions for dual-polarization radar meteorological observations. *J. Atmos. Oceanic Technol.,* **18,** 629–648.

Torlashi, E., and A. R. Holt, 1993: Separation of propagation and backscattering effects in rain for circular polarization diversity S-band radars. *J. Atmos. Oceanic. Technol.,* **10,** 465–477.

——, and ——, 1998: A comparison of different polarization schemes for the radar sensing of precipitation. *Radio Sci.,* **33,** 1335–1352.

——, and Y. Gingras, 2000: Alternate transmission of +45° and −45° slant polarization and simultaneous reception of vertical and horizontal polarization for precipitation measurement. *J. Atmos. Oceanic Technol.,* **17,** 1066–1076.

Vivekanandan, J., D. S. Zrnić, S. M. Ellis, R. Oye, A. V. Ryzhkov, and J. Straka, 1999: Cloud microphysical retrieval using S-band dual-polarization radar measurements. *Bull. Amer. Meteor. Soc.,* **80,** 381–388.

Zrnic, D. S., 1991: Complete polarimetric and Doppler measurements with a single receiver radar. *J. Atmos. Oceanic Technol.,* **8,** 159–165.

——, and A. V. Ryzhkov, 1999: Polarimetry for weather surveillance radars. *Bull. Amer. Meteor. Soc.,* **80,** 389–406.